Dynamic Effects of Temperature Control Tray Location in Distillation Columns

J. P. SHUNTA and W. L. LUYBEN

Lehigh University, Bethlehem, Pennsylvania

This paper presents the results of theoretical and experimental studies of the dynamic effects of varying the location of the temperature control tray in a distillation column. The binary methanol-water system was studied in a 24-tray, 8-in. I.D. column with reflux manipulated to hold the temperature on various trays in the rectifying section of the column.

The ultimate gain and ultimate frequency of the temperature feedback control loops were found to decrease as the temperature control tray was moved down the column away from the top. This confirmed the qualitative statements made by many workers and the quantitative work recently reported by Beaverstock.

The process natural frequency (or breakpoint frequency) was found, unexpectedly, to increase somewhat as the temperature control tray was moved down the column. This meant that the open-loop response of tray liquid composition to reflux flow changes was slightly slower for trays near the top of the column. Because of the increasing purity near the top, adjacent trays differed little in composition and the slope of the equilibrium line was flatter. Both contributed to slower dynamic response.

In developing a theoretical model for the real system studied, the linear model and solution techniques of Lamb, Pigford, and Rippin were extended to include nonequimolal overflow effects.

Theoretically, the best place to locate a temperature sensor to control overhead distillate composition would be on the top tray for a constant-pressure binary system. The temperature would represent the true distillate composition and the lags between the manipulative variable and controlled variable would be minimized.

However, the practical considerations of sensor sensitivity and variable pressures usually require the temperature sensor to be moved down into the rectifying section. The ratio of the change in tray temperature to the change in distillate composition ($\Delta Tc/\Delta X_D$) decreases as the sensor is moved up the column. A point will be reached where the sensor can no longer detect small enough changes to control the distillate satisfactorily. On the other hand, the lower in the column the sensor is located the more steady state deviation in x_D will be experienced. This occurs because the reflux change required to hold the control tray temperature constant will not, in general, be the correct change to hold the distillate composition constant. Thus a design compromise is usually made in determining control tray location.

The steady state aspects of this topic have been discussed in many papers (*1* to *5*). In early investigations sensor sensitivity was lower than it is now, so the criteria for optimum tray location has changed as instrumentation has improved. In addition, the development of pressure-compensated temperature transmitters has removed some restrictions on location of the control tray.

The only study concerned with the dynamic aspects of control tray location is the recently reported work of Beaverstock (*6*). He studied experimentally a closed-loop system with a differential vapor pressure cell sensor near the top of the column for a methanol-water system. Luyben (*7*) studied a combined feed forward/feedback control system with intermediate tray temperatures. He showed that for changes in feed composition, control tray compositions must be changed to keep product compositions constant. The magnitude of the required change increased as the control tray was moved away from the ends of the column.

The purpose of this paper is to present the results of theoretical and experimental studies of the dynamic

TABLE 1. AVERAGE OPERATING CONDITIONS; METHANOL-WATER SYSTEM

System pressure, 1 atm. (assumed throughout column)
Feed rate, 0.705 gal./min.
Feed temperature, 57°C.
Feed composition, 35.27% MeOH
Reflux rate, 0.34 gal./min.
Reflux temperature, 42°C.
Distillate rate, 0.37 gal./min.
Bottoms rate, 0.38 gal./min.
Tray efficiency, approx. 40% in rectifying section; approx. 60% in stripping section
Reboiler holdup, 3.45 gal.
Reflux drum holdup, 1.47 gal.
Condenser holdup, negligible
Reflux piping, 0.656 gal. (assumed plug flow)
Steam line pressure, 70 lb./sq. in. gauge
Calandria steam pressure, 11 lb./sq. in. gauge
Steam flow, 2.77 lb./min.

effects of temperature control tray location. Ultimate gain and ultimate frequency of the feedback control loop were determined for various control trays in the rectifying section. Phase and gain margins for proportional-integral and proportional-integral-derivative controllers using Ziegler-Nichols settings were also compared.

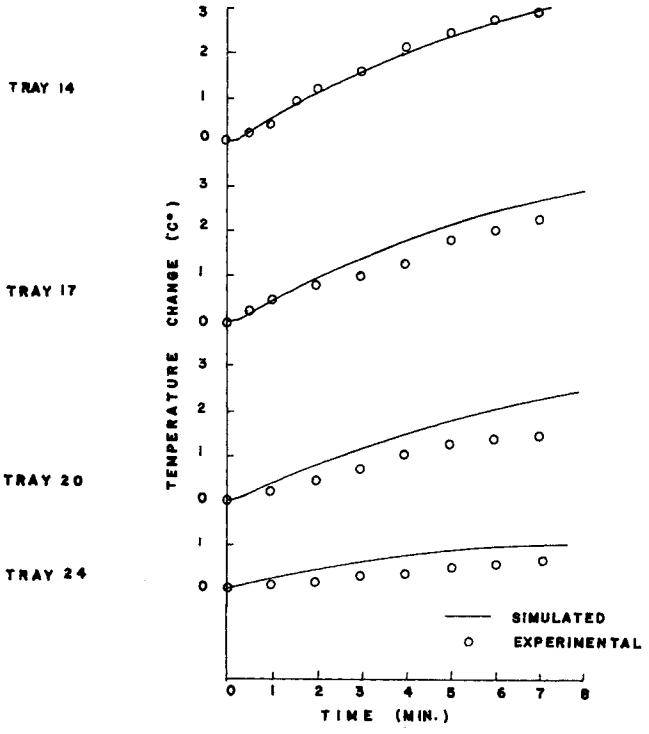

Fig. 2. Comparison of experimental and simulated open-loop response of tray composition.

Experimental System

The binary system methanol-water was studied at atmospheric pressure in a 24-tray, 8-in. I.D. bubble-cap column. The column had a vertical thermosyphon reboiler, feed preheater, and overhead condenser and accumulator system.

As shown in Figure 1, the top temperature was controlled by a pneumatic cascade control system with reflux as the manipulative variable. The column also had a bottom temperature control loop that was not used in this work. Steam was flow controlled. The sensor was a Moore Products Nullmatic (50° to 100°C, range) temperature transmitter. A Princo Densitrol continuously measured reflux density which could be converted to composition. The slave reflux flow controller was a Moore Nullmatic with proportional-reset action. The master temperature controller had proportional, reset, and derivative action. Seven tray temperatures and three stream temperatures were continuously recorded on a Leeds and Northrup Speedomax multipoint temperature recorder.

Feed was introduced onto tray 8. Subcooled reflux returned by gravity flow from the 6-in. × 24-in. vertical reflux drum through an overflow line located halfway up the drum. Average operating conditions are given in Table 1.

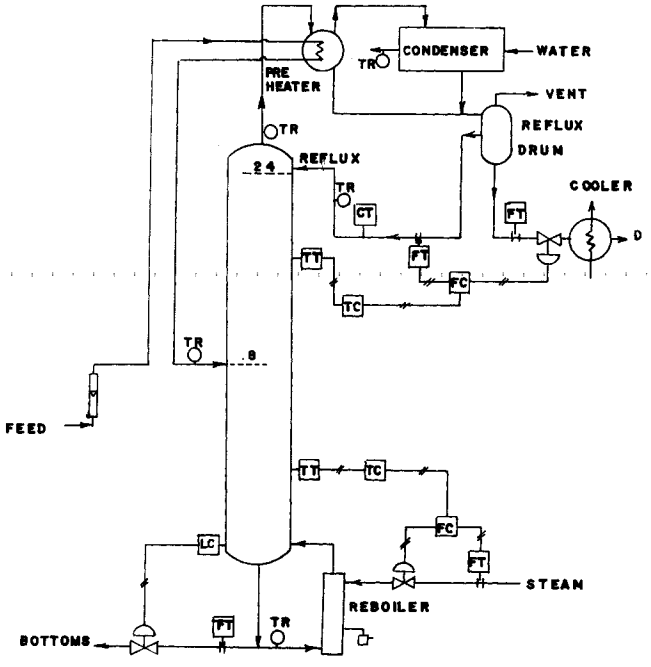

Fig. 1. Lehigh University distillation column and instrumentation.

THEORETICAL MODELS AND COMPUTER SIMULATIONS

Nonlinear

Steady state: A digital computer program was developed to determine steady state conditions for the nonequimolal overflow, nonideal system. Experimental steady state data were used to determine overall tray efficiencies (40% in the rectifying section and 60% in the stripping section).

Dynamic: The nonlinear equations describing the column were simulated on the Lehigh University CDC 6400 digital computer. Theoretical nonlinear open-loop response was compared to experimental results for a step change in reflux flow from 0.39 to 0.32 gal./min. The resulting temperature response curves for trays 14, 17, 20, and 24 (top tray) are shown in Figure 2.

Linear

A digital computer program (NEMO) was developed to solve the system of linearized equations for a nonequimolal overflow column. This program generated Bode plots for the open-loop process transfer functions relating various control tray compositions to reflux flow. The stepping technique of Lamb and Rippin (8) was used with appropriate modification for nonequimolal overflow effects.

NEMO solved the system of linearized distillation equations in the frequency domain by the following method. One of the variables, x_f, F, V_B, B, or x_B was set to the unit impulse, $1 + 0i$, and the rest were set to zero. The

compositions and flow rates were calculated tray by tray from the material and energy balances starting at the reboiler. The procedure was repeated for the other variables. The final simultaneous equations were solved for x_D, x_B, and control tray compositions x_c as functions of F, x_f, V_B, and R at one frequency. The entire procedure was repeated for more frequencies. The steady state program was used to calculate the constant coefficient matrix. A time delay of 2.5 min. was included in the reflux piping.

A nonequimolal overflow system requires an additional differential equation (the energy equation) for each plate.

Nonlinear n^{th} tray equations:

$$\frac{dM_n}{dt} = L_{n+1} + V_{n-1} - L_n - V_n \tag{1}$$

$$\frac{d}{dt}(M_n x_n) = L_{n+1}\, x_{n+1} + V_{n-1}\, Y_{n-1} - L_n x_n - V_n Y_n \tag{2}$$

$$\frac{d}{dt}(M_n h_n) = L_{n+1}\, h_{n+1} + V_{n-1}\, H_{n-1} - L_n h_n - V_n H_n \tag{3}$$

After linearization and using linearized hydraulic and physical property equations

$$Y_n = (\bar{\phi}')\, x_n \tag{4}$$

$$M_n = (\beta_n)\, L_n \tag{5}$$

$$h_n = (\gamma_n{}^L)\, x_n \tag{6}$$

$$H_n = (\gamma_n{}^v)\, Y_n = (\gamma_n{}^v\, \bar{\phi}_n')\, x_n \tag{7}$$

Equations (1) to (3) become

$$\frac{dL_n}{dt} = \frac{1}{\beta_n}(L_{n+1} + V_{n-1} - L_n - V_n) \tag{8}$$

$$\frac{dx_n}{dt} = \left(\frac{\bar{x}_{n+1} - \bar{x}_n}{\bar{M}_n}\right) L_{n+1} + \left(\frac{\bar{x}_n - \bar{Y}_n}{\bar{M}_n}\right) V_n + \left(\frac{\bar{Y}_{n-1} - \bar{x}_n}{\bar{M}_n}\right) V_{n-1} + \left(\frac{\bar{L}_{n+1}}{\bar{M}_n}\right) x_{n+1} - \left(\frac{\bar{L}_n + \bar{V}_n\, \bar{\phi}'_n}{\bar{M}_n}\right) x_n + \left(\frac{\bar{V}_{n-1}\, \bar{\phi}'_{n-1}}{\bar{M}_n}\right) x_{n-1} \tag{9}$$

$$\frac{dx_n}{dt} = \left(\frac{\bar{h}_{n+1} - \bar{h}_n}{\bar{M}_n\, \gamma_n{}^L}\right) L_{n+1} + \left(\frac{\bar{h}_n - \bar{H}_n}{M_n\, \gamma_n{}^L}\right) V_n + \left(\frac{\bar{H}_{n-1} - \bar{h}_n}{\bar{M}_n\, \gamma_n{}^L}\right) V_{n-1} + \left(\frac{\bar{L}_{n+1}\, \gamma^L{}_{n+1}}{\bar{M}_n\, \gamma_n{}^L}\right) x_{n+1} - \left(\frac{\bar{L}_n\, \gamma_n{}^L + \bar{V}_n\, \gamma_n{}^v\, \phi_n'}{\bar{M}_n\, \gamma_n{}^L}\right) x_n + \left(\frac{\bar{V}_{n-1}\, \gamma^v{}_{n-1}\, \phi'_{n-1}}{\bar{M}_n\, \gamma^L{}_n}\right) x_{n-1} \tag{10}$$

Note that in a nonequimolal overflow column, the perturbations in vapor flows on adjacent trays are not equal.

$$V_n \neq V_{n-1} \neq V_{n-2} \tag{11}$$

As one calculates up from the bottom of the column using the stepping technique, at the n^{th} tray the three equations like Equation (8), (9), and (10) can be solved for the three unknowns at that tray: x_{n+1}, L_{n+1}, and V_n.

The calculation procedure is (see 9 for more details):

a. Set x_B, V_B, B, x_f, F (one at a time) equal to the unit impulse and the rest to zero (for one value of frequency w).

b. Calculate x's, L's, V's up the column for each variable.

c. At top of column obtain complex numbers relating x_D, R to each variable:

$$\begin{aligned} x_D &= g_{11}x_B + g_{12}V_B + g_{13}B + g_{14}x_f + g_{15}F \\ R &= g_{21}x_B + g_{22}V_B + g_{23}B + g_{24}x_f + g_{25}F \\ x_D &= g_{31}x_B + g_{32}V_B + g_{33}B + g_{34}x_f + g_{35}F \end{aligned} \tag{12}$$

d. Solve for process transfer functions by solving above three equations simultaneously:

$$\begin{aligned} x_D &= P_{11}x_f + P_{12}F + P_{13}R + P_{14}V_B \\ x_B &= P_{21}x_f + P_{22}F + P_{23}R + P_{24}V_B \end{aligned} \tag{13}$$

e. For designing feedback controllers, the process transfer function x_c/R is calculated as follows:

$$x_c = g_{41}x_B + g_{42}V_B + g_{43}B + g_{44}x_f + g_{45}F \tag{14}$$

Substitute x_B and B from step d and solve for x_c in terms of x_f, F, V_B, and R.

f. Convert composition change x_c to temperature change by using the slope of the $T - x$ curve at 1 atm.

g. Repeat sequence for another value of frequency w.

FEEDBACK CONTROLLER TESTS AND TUNING

Slave Reflux Flow Control Loop

The open-loop transfer function for the reflux flow system was obtained empirically by making a step change in the pressure signal to the control valve as shown in Figure 3. An approximate transfer function was fitted to the resulting response curve of reflux flow.

$$Gv = \frac{Kv\, e^{-Ds}}{Tv\, s + 1} = \frac{-0.35\, e^{-0.117s}}{0.25\, s + 1} \tag{15}$$

A Bode plot was generated for Gv and Zeigler-Nichols settings were determined from the ultimate frequency and ultimate gain. These settings were compared to settings obtained by finding the ultimate gain and frequency experimentally.

	Kc	Ti
Theoretical	5	0.3
Experimental	4.5	0.1

The block diagram for the cascade control loop is shown in Figure 4. The closed-loop transfer function, $BsGv/(1 + BsGv)$, was calculated from $BsGv$.

$$BsGv = \left[\frac{Kc(Ti\, s + 1)}{Ti\, s}\right]\left[\frac{Kv\, e^{-Ds}}{Tv\, s + 1}\right] \tag{16}$$

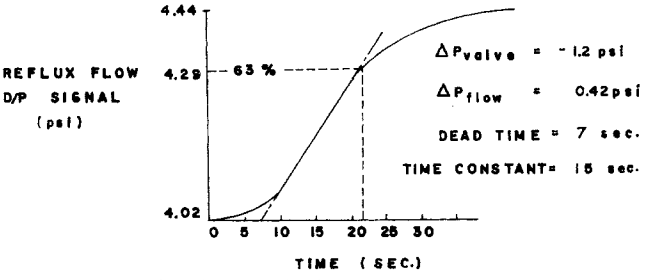

Fig. 3. Control valve response curve.

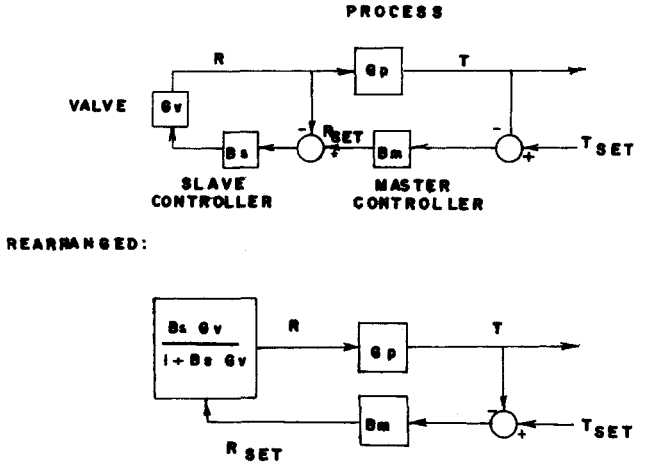

Fig. 4. Cascade control loop.

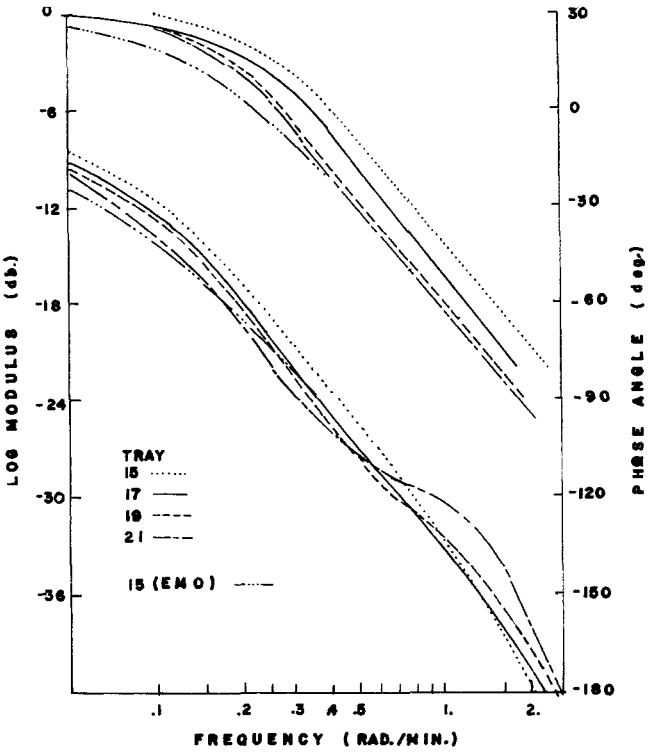

Fig. 5. Control tray process transfer functions.

Master Temperature Control Loop

The open-loop transfer functions Gp between various control tray temperatures and reflux flow were calculated as Bode plots by the NEMO computer program. The total open-loop transfer function for the master loop with the slave loop on control was determined by combining the Bode plots of T_c/R and the closed slave loop transfer function $BsGv/(1 + BsGv)$. The settings for the PI and PID master controller were designed using Ziegler-Nichols techniques for trays 15, 17, 19 and 21. See Table 2.

The settings for tray 17 were determined experimentally and check well with the theoretical results. A measurement delay of 0.47 min. was included in NEMO to match the experimental critical frequency for tray 17. The experimental ultimate gains were determined to be accurate within ± 20%. The ultimate gain and ultimate frequency increased as the sensor was moved up the column. The higher Ku and w_u made the response of the control system more rapid. This result agrees with Beaverstock (*6*).

An interesting and unexpected prediction of NEMO was that the natural frequency ω_n (the frequency at which the magnitude ratio begins to drop off) decreased slightly as one moved up the column. This would mean that the time constant in the open-loop process transfer function increased so that trays close to the top of the column would have a slower response to changes in reflux than do lower ones. The Bode plots from NEMO for several (Tc/R) transfer functions are shown in Figure 5. The phase angles of the higher trays decreased more rapidly for frequencies less than 0.6 rad/min. At higher frequencies the curves crossed and the phase angles for the lower trays decreased faster. (The Bode plot for T_{15}/R for an equimolar overflow model is shown in Figure 5 to compare to the nonequimolar overflow model.)

Experimental results reported by Armstrong and Wood (*10*) tend to verify these results. They found that trays nearer the feed tray approach equilibrium sooner than those at the ends of the column for step changes in reflux.

Because of the increasing purity near the top, adjacent trays differed little in composition and the slope of the equilibrium line was flatter. Both contributed to slower dynamic response.

The Bode plots for the process, closed slave loop, and master controller (with Zeigler-Nichols settings) for trays 15, 17, 19, and 21 were combined and the gain and phase margins were determined. The results are listed in Table 3, for a PI and PID controller. The gain and phase mar-

Table 2. Master Controller Settings by Zeigler-Nichols Criteria

Tray	w_u, rad./min.	Ku	Kc	Ti, min.
	PI Controller			
21	2.5	13.8	6.2	2.2
19	2.3	12.9	5.8	2.3
17	2.1	12.6	5.7	2.5
15	2.0	10.6	4.8	2.7
17 (Experimental)	2.1	12.5	5.6	2.5

Tray	Kc	Ti	Td, min.
	PID Controller		
21	8.3	1.3	0.32
19	7.7	1.4	0.34
17	7.6	1.5	0.38
15	6.4	1.6	0.4

Table 3. Phase and Gain Margins of Open Feedback Loop

Tray	$w(db = 0)$	Phase margin, deg.	$w(\theta = -180°)$	Gain margin, db
	PI Controller			
21	0.92	33	2.6	9
19	0.96	26	1.9	7
17	0.98	21	1.7	6
	PID Controller			
21	1.15	35	3.5	6.5
19	1.15	28	3.3	6.7
17	1.15	27	3.2	6.6

Table 4. Selection of Highest Control Tray from Sensor Sensitivity

	Temperature, °C. Steady state 1 $x_D = 0.95290$	Steady state 2 $x_D = 0.96448$	ΔTn	$\frac{0.0001\ \Delta Tn}{\Delta x_D}$
Tray:				
24	66.06078	65.65455	0.40623	0.00351
23	66.49954	65.99323	0.50631	0.00437
22	66.97904	66.37358	0.60546	*0.00522*
21	67.49751	66.79811	0.69940	0.00604
20	68.05122	67.26805	0.78317	0.00676
19	68.63425	67.78299	0.85126	0.00735
18	69.24193	68.34017	0.90176	0.00779
17	69.87051	68.93632	0.93419	0.00807

gins were not significantly different for either type of controller. It was concluded that the relative stability was about the same for each loop and that the differences in the process natural frequencies did not significantly alter the closed-loop stability.

SENSITIVITY RESTRICTION ON CONTROL TRAY LOCATION

The temperature transmitter had a sensitivity of 0.005°C. (0.01% of the 50° range). The criterion for good control was chosen to be a maximum Δx_D of 0.0001 mole fraction. Therefore the change in control tray temperature for a Δx_D of 0.0001 should exceed 0.005°, assuming that pressure effects have been suitably compensated for. Two steady states were determined for reflux flows of 0.078 and 0.083 mole/min. at the same vapor boilup. Table 4 shows the tray temperatures for each steady state and the temperature differences. The temperature change on tray n for a Δx_D of 0.0001 was

$$\Delta T = 0.0001\ \Delta Tn/\Delta x_D$$

Tray 22 was therefore the highest control tray.

SUMMARY AND CONCLUSIONS

The effect of control tray location on the stability of the feedback loop, process natural frequency, and steady state deviation in x_D for a feed rate disturbance was studied for a methanol-water distillation column. The relative stability of the various feedback loops were not significantly different even though the process natural frequency decreased as the control tray was moved up the column. The controller settings for a cascade control scheme were obtained by Zeigler-Nichols criteria based on the ultimate frequency and ultimate gain of the process. It was found that Ku and w_u increased as the control tray location was moved up the column.

NOTATION

B = bottoms flow rate, moles/min.
Bm = master controller transfer function
Bs = slave controller transfer function
D = dead time, min.
db = log modulus, decibels
F = feed rate, moles/min.
g = transfer function
Gp = process transfer function (T_c/R)
Gv = valve transfer function
H = saturated vapor enthalpy, B.t.u./mole
h = saturated liquid enthalpy, B.t.u./mole
Kc = controller gain
Ku = ultimate gain (K_c at limit of closed-loop stability)
Kv = valve gain
L = liquid flow rate, mole/min.
M = liquid holdup, moles
P = plant transfer function
ΔP = pressure drop, lb./sq.in.
PI = proportional-integral controller
PID = proportional-integral-derivative controller
R = reflux flow, moles/min.
s = Laplace transform variable
T = temperature, °C.
t = time, min.
Td = derivative time, min.
Ti = reset time, min.
Tv = valve time constant, min.
V = vapor flow rate, moles/min.
w_n = natural frequency, w where log modulus is −3 db., rad./min.
w_u = ultimate frequency, w where phase angle is −180 deg., rad./min.
x = mole fraction more volatile component in liquid
Y = mole fraction more volatile component in vapor

Greek Letters

β = hydraulic constant, min.
$\overline{\phi'}$ = slope of equilibrium curve
γ^L = slope of liquid enthalpy versus x curve, B.t.u./mole
γ^v = slope of vapor enthalpy versus Y curve, B.t.u./mole
θ = phase angle, deg.

Subscripts

B = bottoms
c = control tray
f = feed
n = tray number
D = distillate
nT = top tray
Overscore indicates steady state values.

LITERATURE CITED

1. Uitti, K. D., *Instruments*, **23**, 719 (July 1950).
2. Animisov, I. V., "Automatic Control of Rectification Processes," Consultants Bureau (1957).
3. Wood, C. E., *Chem. Eng. Progr.*, **64**, (1), 85 (Jan. 1968).
4. Bertrand, L., and J. B. Jones, *Chem. Eng.*, 139 (Feb. 20, 1961).
5. Rosenbrock, H. H., *Trans. Inst. Chem. Eng.*, **40**, 35 (1962).
6. Beaverstock, M. C., Ph.D. thesis, Cornell Univ., Ithaca, N. Y. (1968).
7. Luyben, W. L., *Chem. Eng. Sci.*, **24**, 997 (1969).
8. Rippin, D. W. T., and D. E. Lamb, paper presented at AIChE Washington, D. C. Meeting (1960).
9. Shunta, J. P., M. S. thesis, Lehigh Univ., Bethlehem, Pa. (1969).
10. Armstrong, W. D., and R. M. Wood, *Trans. Inst. Chem. Eng.*, **39**, 65 (1961).

Manuscript received December 1, 1969; revision received January 16, 1970; paper accepted January 23, 1970.